1-1-2016

Copper Oxide Nanoparticles Inhibit the Metabolic Activity of *Saccharomyces cerevisiae*

Michael Joseph Mashock
Marquette University

Anthony D. Kappell
Marquette University, anthony.kappell@marquette.edu

Nadia Hallaj
Marquette University

Krassimira R. Hristova
Marquette University, krassimira.hristova@marquette.edu

Accepted version. *Environmental Toxicology*, Vol. 35, No. 1 (January 2016): 134-143. DOI.

Copper Oxide Nanoparticles Inhibit the Metabolic Activity of *Saccharomyces cerevisiae*

Michael J. Mashock
Department of Biological Sciences, Marquette University, Milwaukee, WI
Anthony D. Kappell
Department of Biological Sciences, Marquette University, Milwaukee, WI
Nadia Hallaj
Department of Biological Sciences, Marquette University, Milwaukee, WI
Krassimira R. Hristova
Department of Biological Sciences, Marquette University, Milwaukee, WI

Abstract: Copper oxide nanoparticles (CuO NPs) are used increasingly in industrial applications and consumer products and thus may pose risk to human and environmental health. The interaction of CuO NPs with complex media and the impact on cell metabolism when exposed to sublethal concentrations are largely unknown. In the present study, the short-term effects of 2 different sized manufactured CuO NPs on metabolic activity of *Saccharomyces cerevisiae* were studied. The role of released Cu^{2+} during dissolution of NPs in the growth media and the CuO nanostructure were

Environmental Toxicology, Vol 35, No. 1 (January 2016): pg. 134-143. DOI.

considered. Characterization showed that the 28 nm and 64 nm CuO NPs used in the present study have different primary diameter, similar hydrodynamic diameter, and significantly different concentrations of dissolved Cu^{2+} ions in the growth media released from the same initial NP mass. Exposures to CuO NPs or the released Cu^{2+} fraction, at doses that do not have impact on cell viability, showed significant inhibition on *S. cerevisiae* cellular metabolic activity. A greater CuO NP effect on the metabolic activity of *S. cerevisiae* growth under respiring conditions was observed. Under the tested conditions the observed metabolic inhibition from the NPs was not explained fully by the released Cu ions from the dissolving NPs.

Introduction

The novel properties of nanoparticles (NPs) characterized by their small size and unique physical and chemical properties have led to a drastic increase in their incorporation into commercially available products. Copper NPs have uses in gas sensors, batteries, solar cells, catalytic processes, wound dressing, socks, and many other products.[1] The increased use of NPs will predictably lead to accidental introduction into the environment via consumer use or during the manufacturing process. Therefore, the potential of NPs to affect human health and the environment is of significant concern.[2]

The acute toxicity of copper oxide NPs (CuO NPs) has been studied in algae,[3] bacteria,[4] [yeast,[5,6] protozoa,[7] crustacean,[8] and fish[9] species. The extensively used unicellular eukaryotic model organism, *Saccharomyces cerevisiae*, has similar cellular structure and functional organization to those of higher-level organisms[6] making it ideal for use in toxicity studies investigating NPs. Copper cytotoxicity and impact on cellular functions is of intrinsic interest. Copper is biologically essential, and the cellular Cu homeostasis machinery is well conserved between yeast and human.[10] The adverse consequences of defective Cu homeostasis (Wilson's disease and Menkes syndrome in humans) or of changes in external Cu concentration are well documented.[11] Copper oxide NPs have been shown to cause toxicity, such as inhibiting *S. cerevisiae* growth after 24 h of exposure, with the median effective concentration (EC50) ranging from 102 mg Cu/L to 502 mg Cu/L.[5,6] However, limited information is available regarding how dissimilarities in NP characteristics, different exposure conditions, and differences in the metabolic and cell cycle stage of *S. cerevisiae* cultures impact the toxicity metrics. For example, differential Cu resistance has been associated with cell cycle stage and aging in yeast.[12] In addition,

Environmental Toxicology, Vol 35, No. 1 (January 2016): pg. 134-143. DOI.

environmental factors such as ionic strength, pH, and the presence of organic material have an impact on how NPs entering the environment react in solution.[13] Copper oxide NPs have been shown to both dissolve[5,7] and aggregate[9] depending on the conditions within the medium. Some studies have indicated that the acute toxicity observed is due to the release of Cu ions from the NPs.[3,7] However, other studies indicate NP-specific effects.[5,14] Kasemets et al.[6] suggested the observed CuO NP toxicity to a wild-type strain of *S. cerevisiae* was due to a cell surface localized increase in released Cu ions causing an increase in uptake. The authors also suggested in a separate study that the released Cu^{2+} from the CuO NPs could explain approximately half of the toxicity and structure component-related oxidative stress was the mechanism of toxicity.[5] These differing results demonstrate that the toxicity of NPs toward organisms is challenging to predict because of the difficulty of adequately linking the nano-material properties in a directly proportional relationship to the toxic mechanisms. As such, further investigation remains necessary.[15]

The present study investigates the impact of organic molecules-rich growth media on CuO NP dissolution, aggregation, and Cu bioavailability on cellular metabolic activity of *S. cerevisiae*. Cells were exposed to 2 NPs with identical CuO composition but different primary particle size, crystal lattice structure, and amount of released Cu^{2+} after incubation in the growth medium. These CuO NPs were applied as either fresh suspensions or aged NPs in the culture medium. To distinguish between the role of Cu^{2+} ions released from the NPs and the nano-specific effect, parallel exposures were carried out with the released Cu^{2+} fraction in the media from CuO NPs and the NP suspensions. Experiments performed in organic-rich media can represent the diverse and dynamic surroundings that may be encountered with accidental introduction of NPs into the environment,[16] thereby stressing the importance of the role of the experimental media on the cell–NP interactions.

Environmental Toxicology, Vol 35, No. 1 (January 2016): pg. 134-143. DOI.

Materials and Methods

Saccharomyces cerevisiae *strains and cultivation conditions*

Saccharomyces cerevisiae W303-1A wild type (*MAT*a: *leu2-3,112 trp1-1 can1-100 ura3-1 ade2-1 his3-11,15*) was a kind gift of Dr. Rosemary Stuart (Marquette University). The strain was maintained on YP agar plates (pH 6.6) containing 1% yeast extract (Amresco), 2% Bacto peptone (Difco Laboratories), and 2% of the respective carbon source at 30 °C overnight. To prepare starter cultures, single colonies from the respective master plates were transferred in 5 mL YP media with ethanol, galactose, or dextrose as the carbon source and grown overnight at 30 °C with 250 rpm shaking to culture the cells under respiratory, respiratory/fermentative, or fermentative metabolism, respectively. The YP media with dextrose or ethanol as a carbon source were employed to examine the influence of different types of metabolism (fermentation vs respiration) on *S. cerevisiae* sensitivity to Cu treatments, whereas the YP with galactose (fermentation/respiratory metabolism) was employed for all other experiments throughout the present study. *Saccharomyces cerevisiae* experimental cultures were started from the overnight cultures. The turbidity of the cell culture was measured via absorbance at 600 nm using a spectrophotometer (Molecular Devices) and diluted with sterile YP media with respective carbon source to an OD_{600} 0.1. The cultures were grown until OD_{600} 0.3 was reached ($\sim 4.0 \times 10^6$ Colony Forming Units/mL determined by dilutions and plating on YP-galactose plates with colony counting after 72 h at 30 °C incubation). This concentration of cells was consistently used in all toxicity assays. Exposure to tested chemicals was performed in 96-well black with clear bottom, polystyrene plates (Costar) at 30 °C with continuous shaking at 250 rpm.

NP physicochemical characterization

NP diameter and morphology

Bare, uncoated CuO NPs were purchased from Meliorum Technologies (28 nm CuO NPs) or Sigma Aldrich (64 nm CuO NPs).

Environmental Toxicology, Vol 35, No. 1 (January 2016): pg. 134-143. DOI.

Transmission electron microscopy (TEM) was employed to characterize both CuO NPs morphology and primary particle diameter. Diluted CuO NPs suspensions in water or YP-galactose media were deposited onto Cu 200 mesh formvar coated grids and allowed to settle for 10 min prior to removal of the excess liquid. Transmission electron microscope imaging was performed on a Hitachi H9000NAR Analytical High Resolution TEM, 300 KeV (dpr) and the primary particle diameters were assessed using ImageJ image processing and analysis software. Briefly, the measuring tool was employed after altering the scale to nanometers, to assess dimensions of 100 individual NPs of both 28 nm and 64 nm CuO NPs in 15 or more images. Measurement of NPs diameter was performed only when well-defined individual NPs could be observed. Transmission electron microscope micrographs of gold NPs at established dimensions were analyzed in identical fashion with ImageJ to confirm validity of measurements (data not shown).

NP dispersion

A stock solution of CuO NPs (8000 mg/L) was prepared in sterile deionized water and dispersed by using a 450 W probe sonicator (Branson Digital Sonifer) at 20% amplitude for 5 min on ice with pulsing on for 20 s and off for 20 s. The stock solutions were stored in the dark at an ambient temperature. After 5 min dispersion, different volumes of the CuO NPs stock solution were aseptically added to yeast cultures (in YP medium containing different carbon sources) to achieve different exposure concentrations.

NP hydrodynamic diameter and zeta potential

To determine the average hydrodynamic diameters of CuO NPs agglomerates, NPs were diluted to 40 mg/L in sterile double distilled water (ddH_2O) or growth medium (YP-galactose) and injected using a sterile syringe into the viewing chamber of NS500 platform (Nanosight) equipped with a 640-nm laser. All measurements were taken at room temperature. Average diameters and standard deviations were measured using the nanoparticle tracking analysis (NTA) 2.0 Build 127 analytical software for real-time dynamic NP visualization and measurement. The samples were measured for 30 s with manual shutter and gain adjustments, and 6 measurements of the same sample were performed for all of the respective time points.

Environmental Toxicology, Vol 35, No. 1 (January 2016): pg. 134-143. DOI.

Although Nanosight has a minimum limit of detection of 10 nm, the smaller CuO NPs employed in the present study have an average primary particle diameter, as measured by TEM, of 28 nm. However, it should be noted that any populations of CuO NPs or agglomerations smaller than 10 nm would not be detected by NTA. To exclude artifacts from organic components within media, analysis of YP growth media without adding CuO NPs was performed and run in batch processing as 5 separate runs to avoid introducing additional artifacts from altering fluidic flow. The data were combined and averaged to provide background intensity data, which was then used to exclude organic matter from conflicting with the NPs/organic matter agglomeration measurements. This exclusion was accomplished through the use of the "intensity comparison" tool in the NTA 2.0 Build software, which allows the user to establish intensity values as a cutoff for the minimal intensity necessary to be incorporated in the sample analysis. To determine Zeta potentials of CuO NPs in YP media, NPs in solution were pipetted into Folded Capillary Cells (Malvern Instruments) and Zeta potential was measured using a Zetasizer Nano-ZS (Malvern Instruments).

NP aging in the growth media

Note that *S. cerevisiae* has a high Cu tolerance, up to 480 mg/L CuO NPs for 12 h of exposure in YP media before lethal effects are observed (data not shown). In the present study, sublethal NP concentrations in the range of 40 mg/L to 240 mg/L were employed in 1.5 h exposure scenario to study the NPs' effect on *S. cerevisiae* cell metabolism. To explore media component-NP interactions, CuO NPs were dispersed into YP-galactose media as described above in *NP dispersion* to 40 mg/L, 80 mg/L, or 240 mg/L initial mass in 4 mL volume in 15-mL polypropylene disposable centrifuge tubes (VWR). The NP solutions were covered to prevent light exposure and placed at 30 °C in a table-top shaking incubator at 250 rpm for 24 h. A 2-mL aliquot of the "aged" NPs were ultracentrifuged at 45 000 g for 30 min (Optima MAX-E Ultracentrifuge) and supernatant was then removed and used as released fraction. The CuO NP pellet was resuspended in sterile YP-galactose media and used as aged NPs in fresh media. The remaining 2 mL of aged NPs in released fraction was used as an additional treatment. Fresh suspensions of CuO NPs were prepared by

diluting stock solution (8000 mg/L) to 40 mg/L, 80 mg/L, and 240 mg/L and immediately added to cell suspensions for exposure.

In cases of NP exposure with Cu^{2+} chelation, ethylenediaminetetraacetic acid (EDTA) in a final concentration of 0.5 mM was added to CuO NPs or the released ionic Cu fraction in YP-galactose medium and incubated at 30 °C for 1 h prior to adding *S. cerevisiae* cells. The *S. cerevisiae* cells used as the untreated control were pelleted and resuspended in growth media, which was also supplemented with EDTA.

NP dissolution

To define the amount of Cu^{2+} ions released from CuO NPs in the growth media, aliquots of each NP suspension in YP-galactose medium were collected immediately after dispersion in the media, after 1.5 h or 24 h incubation at 30 °C with shaking (250 rpm) and ultracentrifuged (45 000 *g* for 30 min) to remove cells and suspended CuO NPs. Aliquots were stored at 4 °C (up to 1 wk) until Zincon analysis was performed. The Cu^{2+} ion concentration was measured using Zincon assay as described by Sabel et al.[17] with the following modifications: Measurement of Cu^{2+} within the supernatant was performed on a Spectra Max M2e spectrophotometer (Molecular Devices) using Zincon reagent (MP Biochemicals). All samples were diluted in Tris–HCl buffer (20 µM, pH 7.2) containing Zincon (40 µM). A standard curve with Cu^{2+} (0–2.4 mg/L) was prepared from $CuSO_4$ in the same buffer. Samples were incubated at room temperature for 10 min and absorbance was measured at 615 nm. The relationship between absorbance at 615 nm and the known concentration of Cu^{2+} standard served to determine Cu^{2+} ion concentration. To observe the influence of organic material and anions, identical experiments were performed in double distilled water. To remove the pH as a potential variable, distilled water was adjusted to pH 6.4, identical to the growth media. Prior to analysis the supernatants were examined for the presence of NPs using NTA; we concluded that NPs were not detectable. Nanoparticles with a diameter less than 10 nm were not detected due to the limit of detection by NTA, but they still may have been present. However, even if a small NP fraction of <10 nm is present, preliminary experiments indicate that

Environmental Toxicology, Vol 35, No. 1 (January 2016): pg. 134-143. DOI.

Zincon dye does not interact directly with CuO NPs (data not shown). All measurements were performed in triplicate.

To define the amount of total Cu released from CuO NPs in the growth media, aliquots of previously ultracentrifuged supernatant was digested with equal volume 70% (w/v) HNO_3 at 65 °C for 2 h and stored in acid-washed glass vials at 4 °C for no more than 1 wk. Samples were then further diluted to 2% HNO_3 with ddH_2O, containing 0.5% HCL, prior to sample analysis using inductively coupled plasma mass spectrometry (7700 × ICP-MS with autosampler, Agilent Technologies). Inductively coupled plasma mass spectrometry detects total Cu regardless of Cu ion species, Cu in strong-association with organic material, or Cu in the form of nano-solids.

Cell viability spot assay

Overnight cultures of *S. cerevisiae* in YP-galactose media were diluted to OD_{600} 0.1 and 150 µL of the cell suspensions were aliquoted to 0.6 mL 96-deep-well plate. Cell suspensions were mixed with 150 µL of CuO NPs and $CuSO_4$ solutions in YP-galactose media. Plates were covered loosely with aluminum foil and incubated at 30 °C for 24 h with shaking at 250 rpm. Cells were then serially diluted in PBS buffer (pH 7.2) and 2 µL of the cell solutions were spotted onto YP-galactose agar plates in triplicate. The formation of colonies was examined visually after 72 h of incubation at 30 °C and was compared with colony formation of untreated cells.

Metabolic activity assay

The inhibitory effects of CuO NPs were determined by quantifying cellular metabolic activity using alamarBlue (aB, Invitrogen), a cell-permeable redox-sensitive dye that turns from a nonfluorescent blue color to a highly fluorescent pink color on reduction by metabolically active cells. Fluorescence detection of the reduced aB signal was performed in a Spectra Max M2e spectrophotometer (Molecular Devices).

Metabolic activity assay was performed according to the following protocol: Cu treatments were generated by adding $CuSO_4$,

released Cu^{2+} fraction from NPs, or dispersed CuO NPs into YP-galactose media to achieve 300 µL volume at the desired concentration. Freshly inoculated cultures of *S. cerevisiae* in YP-galactose media were incubated at 30 °C for 3 h to 4 h until OD_{600} 0.3 was reached, centrifuged at 4000 rpm for 2 min, the supernatant was removed, and the cell pellets were then resuspended with YP-galactose media containing different Cu compound. Each experimental treatment was amended with 10% (v/v) alamarBlue dye to achieve a final volume of 330 µL, which was then aliquoted to 3 separate wells to a final volume of 100 µL per well in a 96-well plate (Costar polystyrene flat bottom, nontreated, black sided, clear bottom). Cell-free YP-galactose media was added to cell-free control wells for background subtraction. Plates were covered with aluminum foil to prevent light exposure and incubated at 30 °C, with shaking at 250 rpm for 1.5 h. Fluorescence was recorded at 550 nm/585 nm excitation/emission with a 570 nm cutoff every 5 min for 1.5 h. Cellular metabolic rate was determined by employing SpectraMax software to calculate the rate of fluorescence at the linear portion of each curve. Each respective treatment was performed in triplicate wells, and the results were averaged per well. Data were the mean of 3 independent experiments plus or minus the standard deviation.

Preparing released fraction exposure scenario

When $CuSO_4$ was used to mimic the released Cu^{2+} from CuO NPs, less metabolic inhibition was observed compared with exposure with the actual released fraction from NPs (Supplemental Data, Figure S1). This observation of soluble Cu salt treatments not being an adequate mimic of NP-released Cu ion treatment has also been reported in other studies.[16] Only after incubating $CuSO_4$ in YP-galactose (to simulate the Cu ions released from CuO NPs) was the metabolic inhibition more similar to the metabolic inhibition observed with released Cu treatments (Supplemental Data, Figure S2). Instead of aged $CuSO_4$, the released Cu ion-containing supernatant from the CuO NPs was used in the subsequent experiments to represent the nature of the soluble Cu within the YP-galactose media more effectively. To characterize the released Cu from CuO in the growth media, total Cu was measured with ICP-MS. In the "released Cu only" exposure scenario Cu^{2+} is a dominant fraction because the

concentration of total Cu, as measured with ICP-MS, was not significantly different than Cu^{2+} ions concentrations, as measured with zincon assay (Supplemental Data, Figure S3).

Statistical analysis

For all data, significant differences between samples were determined using pair-wise comparisons performed by *t*-test (after confirming normal distribution), and *p* values of less than 0.05 were considered significant. The chemical concentration necessary to reduce cell metabolic activity by 50% (IC50) was determined by comparing treated values to the untreated using the log-normal model in the Excel macro REGTOX.[18]

RESULTS

CuO NP characterization

Copper oxide NPs from 2 different commercial sources were characterized for primary NP diameter and morphology by TEM (Figure 1 E–H). The Meliorum CuO NPs have an average primary particle diameter of 28.4 nm, referred to as 28 nm CuO NPs in the present study, whereas the Sigma CuO NPs had an average primary particle diameter of 64.2 nm, herein referred to as 64 nm CuO NPs (Figures 1G and 1H). The 28 nm CuO NPs displayed a rough surface, spherical shape, and a uniform size distribution (large black arrows, Figures 1E and 1F). Transmission electron microscopy imaging of the 64 nm CuO NPs showed different morphologies with both small spherical particles and large irregular crystals being observed in the same sample (Figure 1G). The 28 nm and 64 nm CuO NPs exhibited a purity of > 99.8% as reported by the manufacturers and determined by ICP-MS analysis (data not shown). High-resolution TEM (Figure 1F) images displayed a distance of 2.4 Å between parallel lattice fringes (parallel to solid black lines with small arrows) in the 28 nm CuO NPs, consistent with the spacing of the (2 0 0) crystal planes of CuO. The high-resolution TEM images of 64 nm CuO NPs had parallel lattice fringe spacing of 5.1 Å (Figure 1H) consistent with the interlayer separation of the (1 0 0) crystal plane of CuO.

Environmental Toxicology, Vol 35, No. 1 (January 2016): pg. 134-143. DOI.

Hydrodynamic diameter and zeta potential were measured to determine the propensity of the 28 nm and 64 nm CuO NP to form aggregates or agglomerates (Figure 1 and Supplemental Data, Table S1). Both CuO NPs form similarly sized aggregates when suspended in double distilled water (ddH_2O, Figures 1A and 1B) and similarly sized agglomerates when suspended in YP-galactose growth medium (Figure 1C and 1D). The CuO NPs suspended in water had a significantly smaller hydrodynamic diameter compared with NPs suspended in growth media at pH 6.4 ($p < 0.05$). Although the pH was the same, the ionic strength was significantly higher within YP media compared to water (data not shown). Both increased ionic strength and organic matter have been implicated in increased NP dissolution,[13,19] which may partially explain the increased dissolution observed in YP media compared to water. The 28 nm CuO NPs had an average hydrodynamic diameter of 94 nm when suspended in water and 214.1 nm in YP-galactose medium and in both cases these diameters were smaller than the 64 nm CuO NPs (146.3 nm in water and 246.9 nm in YP-galactose, Figure 1 and Supplemental Data, Table S1). All particles had low zeta potential values (−5.6 to −14.5 mV, Supplemental Data, Table S1) indicating substantial instability and a high potential to form agglomerates in the growth media. Suspensions from both NPs did not alter the pH of the YP-galactose culture medium up to 24 h of incubation (data not shown).

CuO NP dissolution

For nanomaterials, metal ion release is a critical physical parameter; as such, NP dissolution has been suggested to be just as important as surface-dependent effects regarding potential toxicity of nanomaterials.[20] In the present study, the culture media, YP-galactose, led to enhanced CuO NP dissolution compared with water, whereas the smaller 28 nm CuO NPs exhibited greater dissolution than the 64 nm CuO NPs. We observed that distilled water (pH 6.4) had no effect on NP dissolution for most of the exposure doses employed (Table 1) except under prolonged incubation (25.5 h) with higher initial mass of 64 nm particles. The 28 nm freshly resuspended CuO NPs showed higher release of Cu^{2+} in the YP-galactose medium compared with the Cu^{2+} released from the same initial mass of freshly resuspended 64 nm CuO NPs (Table 1). The 28 nm CuO NPs suspended

Environmental Toxicology, Vol 35, No. 1 (January 2016): pg. 134-143. DOI.

in YP-galactose medium displayed up to 21.8% reduction of the initial particle mass, whereas the 64 nm CuO NPs displayed significantly less particle mass loss (2%, $p < 0.01$). The increased CuO NPs dissolution in YP-galactose is in agreement with previous reports indicating enhanced CuO NPs dissolution in culture media containing amino acid-rich components, such as tryptone and yeast extract, compared with dissolution in water.[16,21]

To observe the effects of prolonged media interactions with CuO NPs on dissolution, the 28 nm and 64 nm CuO NPs were suspended in YP-galactose medium for 24 h at 30 °C followed by separation of the remaining CuO solids ("aged" NPs) from the media ("released" Cu^{2+}). Aged 28 nm CuO NPs were pelleted and resuspended in fresh YP-galactose media, which resulted in significantly greater ($p < 0.05$) Cu^{2+} release compared with fresh suspensions of CuO NPs (Table 1). The opposite trend was observed for aged 64 nm CuO NPs in fresh media, which released less Cu^{2+} into YP-galactose compared to fresh suspensions of 64 nm CuO NPs (at 80 mg/L and 240 mg/L, Table 1).

Both CuO NPs used in the present study have different primary NP diameters and different crystal structures (determined by high resolution TEM, Figure 1), similar hydrodynamic diameter (NTA, Figure 1), and released significantly different amounts of Cu^{2+} into the growth media from the same initial NP mass (Table 1).

CuO NPs inhibit S. cerevisiae metabolism

The potential cytotoxicity of 2 different commercially available CuO NPs to *S. cerevisiae* was evaluated using a cell viability spot assay and cellular metabolic activity was assayed by alamarBlue (aB) fluorescence. After 1.5 h and 24 h of exposure, no significant effects on cell viability were observed for the 28 nm and 64 nm CuO NPs up to the highest dose tested (480 mg/L; Supplemental Data, Figure S4). Susceptibility to CuO NPs or $CuSO_4$ exposures was greater in cell cultures undergoing respiratory compared to fermentative metabolism (Table 2). The 1.5 h IC50 values for inhibition of metabolic rate of *S. cerevisiae* W303-1A exposed to 28 nm and 64 nm CuO NPs (fresh suspensions) in the present study were 306 ± 67 mg/L and 467 ± 7 mg/L, respectively, when cultured on YP-dextrose, a fermentative carbon source. These values are consistent with the

Environmental Toxicology, Vol 35, No. 1 (January 2016): pg. 134-143. DOI.

range of the previously reported 24 h growth inhibition test IC50 for *S. cerevisiae* BY4741 of 643 ± 52 mg/L CuO NPs in YP-dextrose medium.[6] *Saccharomyces cerevisiae* cells cultured with respiratory carbon sources, including YP-ethanol, were more sensitive to exposures than cells in fermentative conditions ($p < 0.05$, Table 2). The metabolic rate IC50 for cells on respiratory carbon sources (ethanol and glycerol) are 2 to 5 times lower ($p < 0.01$) compared with exposure to cells cultured on YP-dextrose (fermentative metabolism, Table 2). The IC50 for $CuSO_4$ exposure was more than 20 times lower compared to the IC50 for both CuO NPs in the present study (Table 2). Cells cultured on YP-galactose (fermentative/respiratory carbon source) showed similar or slightly higher sensitivity to CuO NPs and Cu^{2+} exposures compared with YP-ethanol grown cells. In the following experiments YP-galactose was employed because of the higher *S. cerevisiae* W303-1A biomass yield on galactose compared to yield with YP-ethanol (data not shown).

The metabolic state of *S. cerevisiae* had an impact on the degree of inhibition of metabolic activity by Cu treatments. Regardless of the state of metabolism, Cu^{2+} (tested as $CuSO_4$) had greater inhibitory effect than 28 nm CuO NPs followed by the 64 nm CuO NPs.

CuO NP aging on yeast metabolism

To unravel the toxic effect of released Cu^{2+} from that of the CuO NPs, *S. cerevisiae* cells were exposed for 1.5 h to several Cu exposure scenarios: fresh suspensions of NPs in YP-galactose media, aged NPs resuspended in fresh media, aged NPs within YP-galactose containing the released fraction, or the released fraction in YP-galactose without NPs (Figure 2). Among all exposure conditions, 28 nm CuO NPs inhibited *S. cerevisiae* metabolism to a greater extent than 64 nm CuO NPs exposures (Figure 2). The increased inhibitory effect of the 28 nm compared with the 64 nm CuO NPs is consistent with previous studies that frequently show greater toxicity from NPs with smaller primary particle diameter.[22,23]

The aged 28 nm and 64 nm CuO NPs within released fraction and the released fraction in the absence of CuO NPs were significantly ($p < 0.05$) more inhibitory of *S. cerevisiae* metabolic activity compared with exposure to the fresh suspensions of aged CuO NPs in YP-

Environmental Toxicology, Vol 35, No. 1 (January 2016): pg. 134-143. DOI.

galactose media (excluding 64 nm CuO NPs at 40 mg/L, Figure 2). The higher inhibitions of metabolic activity of *S. cerevisiae* were observed in exposure conditions with greater amounts of Cu^{2+}. These results suggest that the presence of greater amounts of released Cu ions, including the measured Cu^{2+} form, had increased toxic effect on *S. cerevisiae* in the presence or absence of CuO NPs compared with freshly resuspended CuO NPs, containing lower amounts of Cu^{2+} (Figure 2).

The aged 64 nm CuO NPs after resuspension in fresh YP-galactose showed significantly greater metabolic inhibition ($p < 0.01$) at initial mass of 80 mg/L compared with 40 mg/L in the presence of similar concentrations of released Cu^{2+} (Table 1 and Figure 2). The observed dose-dependent effect of aged CuO NPs at similar concentrations of released Cu^{2+} indicates the decrease in metabolic activity observed in aged 64 nm CuO NPs treatment is due to the NP component.

The difference in metabolic rate inhibition from freshly resuspended and aged NPs, and the presence of the released Cu^{2+} fractions suggest that both the released Cu ions as well as the CuO NP component have a role in the observed impact on *S. cerevisiae* metabolism.

Effect of chelating Cu ions in NP exposure scenarios

Chelation of Cu^{2+} ions by EDTA addition significantly decreased the metabolic inhibition by aged 28 nm CuO NPs within the released Cu fraction ($p < 0.05$) and the released Cu fraction in the absence of 28 nm or 64 nm CuO NPs ($p < 0.05$, $p < 0.01$, respectively; Figure 3). There was no significant difference of metabolic activity of *S. cerevisiae* in the presence of EDTA of freshly resuspended and aged 28 nm and 64 nm CuO NPs in fresh YP-galactose media nor the aged 64 nm CuO NPs within media containing the released Cu fraction. The observation that under low concentrations of Cu^{2+} present in the NPs exposure scenarios, the addition of EDTA caused no significant change in metabolic activity may suggest that the toxicity observed was due to the NP component.

Chelation of Cu ions with EDTA often resulted in a decrease in inhibition (10–30% decrease of metabolic inhibition with 28 nm and 64 nm CuO NPs exposure scenarios containing the released fraction), although not a complete recovery of cellular metabolic activity. This may be explained by the possibility that the chelation of Cu^{2+} ions may not affect the bioavailability of Cu^{2+} ions to *S. cerevisiae* cells. A study performed by Mei Li et al. in 2013 with ZnO NPs and Zn^{2+} ions suggests that a decrease in free metal ions does not necessarily result in a subsequent decrease in the bioavailable ions that can interact with cells.[24]

The chelation of Cu^{2+} did result in a dramatic reduction in toxicity of several CuO NP exposure scenarios, though not a complete recovery, suggesting that both the released Cu ions as well as the CuO NP component have a role in the observed inhibition of cellular metabolic activity.

Discussion

The physiochemical properties of nanomaterials, such as aggregation, zeta-potential, crystal structure, roughness, primary particle size, agglomeration, and dissolution have been shown to be a factor in relation to their potential cytotoxicity.[13,19,20] We examined the impact of CuO NPs with measured differences in primary particle size, crystal structure, and rate of dissolution in the growth media on *S. cerevisiae* cellular metabolic rate.

The commercially available 28 nm and 64 nm CuO NPs used in the present study were characterized using TEM, Zetasizer, and NTA. Transmission electron microscopy has the advantage of providing a direct image of particle size and morphology at high resolution (Figure 1). The 28 nm CuO NPs appeared as spherical with an average primary particle diameter of 28.4 nm with a range from 17.3 nm to 39.5 nm and the 64 nm CuO NPs had irregular shapes with a small population of NPs showing spherical shapes with an average particle diameter of 64.2 nm within a range of 11.7 nm to 120.7 nm. Catalytic properties, specifically structure-sensitive reactions usually involving oxygen–oxygen bonds, are dependent on particle size.[25,26] The CuO NPs used in the present study also demonstrated similar rough surfaces, which have been associated with differences in the amount and identity of

proteins absorbed on the NP surface.[27] The 28 nm and 64 nm CuO NPs showed different orientations of crystal planes on the surface of the NPs, which may have implications in the available catalytic sites, as implicated with TiO_2 NPs.[28,29] Both CuO NPs used in the present study had similar low zeta-potentials (Supplemental Data, Table S1), indicating the CuO NPs had equal potential to form aggregates and agglomerates in the growth media.[30]

In complement to the TEM, NTA was used to measure particle size in solution in real time with the advantage of needing little to no sample preparation (Figure 1). The NTA software permits the measurement of single NPs, aggregates, or agglomerates in solution greater than 10 nm in size.[31] Aggregation of CuO NPs, as determined in water after sonication, showed greater hydrodynamic diameter in both CuO NPs compared with the primary particle size. Aggregation of uncoated and unmodified oxide NPs is considered to be an intrinsic property.[32,33] The lack of dispersal of the CuO NPs by sonication suggests either fusion or strong bonding of the primary particles or reformation of aggregates after dispersal.[32] Agglomerations consist of interactions between NPs, aggregates of NPs, and media components generating formation of clumps or clusters of primary particles and organic molecules. The CuO NPs within the growth media used in the present study displayed hydrodynamic diameters greater than in water and greater than the primary particle diameter, indicating formation of agglomerates. The aggregation and agglomeration observed in the present study has been reported elsewhere for CuO in water,[6,19] yeast growth media,[6] in the presence of small amounts of organic material,[26] and several different natural waters.[19] Aggregation and agglomeration are important attributes to measure as they decrease the available NP surface area that facilitates interaction with living cells and media components.

The effect of particle size on dissolution was investigated by comparing Cu^{2+} ions released from 28 nm and 64 nm CuO NPs within double distilled water and the complex biological media used in the present study (Table 1). The dissolution of the CuO NPs showed that only a small fraction (3.6%) of the CuO NPs dissolute within the 1.5 h after addition to the growth media. After 24 h within the media, the dissolute concentration of the CuO NPs increased to as much as 52.7%. The observed dissolution of Cu from CuO NPs was consistent

with results reported elsewhere for growth media rich in organic material[34,35] The 28 nm CuO NPs showed greater dissolution than 64 nm CuO NPs. Differences in the amount of Cu ions released from different sized CuO NPs have been described elsewhere.[16] The Ostwald-Freundlich equation predicts that as particle size decreases the equilibrium solubility of particles increases, therefore, smaller NPs would have a greater propensity for dissolution.[36] Factors such as surface curvature and roughness, in addition to size which effects surface area, may also play a role in dissolution of NPs.[36] The size dependent dissolution observed in the present study may be related to the greater surface area with, and particle number of, the 28 nm CuO NP compared with 64 nm CuO NP at equal mass.[37] The difference in exposed crystal structures of 28 nm and 64 nm CuO NPs on the surface may also be leading to different surface chemistries with more reaction sites and thus result in different amounts of Cu^{2+} ion release.[29]

The IC50 for the acute inhibitory effect of CuO NPs and $CuSO_4$ to *S. cerevisiae* metabolic activity were compared (Table 2). The exposure to increasing concentrations of CuO NPs and Cu salt led to decrease in metabolic activity (Supplemental Data, Table S2). When exposure occurred in YP-galactose, Cu salt had significantly greater effect on metabolic activity (IC50: 0.96 mg Cu/L) compared with the 28 nm CuO NPs (IC50: 70.3 mg Cu/L) which were subsequently more toxic than 64 nm CuO NPs (IC50: 172.6 mg Cu/L). *Saccharomyces cerevisiae* under respiratory conditions were more sensitive to CuO NPs exposures compared with fermentative conditions which may implicate respiratory metabolism or the mitochondria in facilitating CuO NP toxicity, as suggested with gold NPs,[38] however we have no direct evidence if this is the case. The lower toxic effect of CuO NPs compared with Cu salts has been shown in the gram-negative bacteria *Escherichia coli*[4] and *Vibrio fischeri,*[39] the protozoa *Tetrahymena thermophile,*[7] and the freshwater crustacean *Thamnocephalus platyurus*.[39] In the present study, *S. cerevisiae* demonstrated greater resistance to the toxicity of the CuO NPs compared with the reported EC50 of the microalgae *Pseudokirchneriella subcapitata* (0.57 mg Cu/L,[3]) and the crustacean *T. platyurus* (1.7 mg Cu/L,[39]). However, the range of concentrations used is similar to other studies as indicated by similar EC50s found in the protozoa *T. thermophila* (127 mg Cu/L,[7]), the bacterium *Bacillus subtillis* (48.8 mg Cu/L [34]), and *Streptococcus aureus* (52.5 mg Cu/L[3]). The observed size dependent metabolic

inhibition of smaller primary particle size yielding greater toxicity is consistent among metal oxide NPs.[16,22] The inhibitory effect due to differences in primary particle size is confounded by the release of Cu^{2+} ions through dissolution, which is greater in the 28 nm CuO NPs compared with the 64 nm CuO NPs, which may explain the increase in impact on cellular metabolic activity.

To unravel the inhibitory effect of the released soluble Cu and that of the structural NP component, the 28 nm and 64 nm CuO NPs were resuspended in the growth media for 24 h prior to separating the remaining NPs and the released Cu ions in solution. *Saccharomyces cerevisiae* was then exposed to freshly resuspended CuO NPs, the aged CuO NPs within the growth media containing the released Cu^{2+}, the aged CuO NPs separated from the released Cu^{2+}, and the growth media containing the released Cu ions in the absence of NPs. The 64 nm CuO NPs freshly resuspended in growth media, independent of aging, showed increased cellular metabolic inhibition with increased NPs mass between 40 mg/L and 80 mg/L despite similar release of Cu^{2+} (Figure 2) indicating that the increased effect on metabolic activity was due to the presence of more NPs. Although 28 nm CuO NPs showed a similar increase in measured inhibitory effect with greater concentration of NPs at similar concentrations of Cu^{2+} released in the fresh media, the increase was not statistically significant. The soluble Cu ions released from CuO NPs did not fully explain the observed toxicity to *S. cerevisiae*, as also observed by Kasemets et al.[5]

Metabolic activity inhibited by CuO NPs was recovered by chelation of Cu ions with EDTA (Figure 3). The recovered metabolic activity from chelation was more dominant in 64 nm CuO NP compared to 28 nm CuO NPs. However, the presence of EDTA did not remove the metabolic inhibition of the aged or freshly resuspended NPs in media with low amounts of soluble Cu. This indicated that the NPs were the cause of the observed effect at the lower dose of exposure. Combined, these results suggest that the observed CuO NPs inhibition of *S. cerevisiae* cell metabolic activity is related to both the NP as well as the dissolute Cu ions. Although the 28 nm CuO NPs showed greater inhibitory effect compared with 64 nm CuO NPs, this is most likely due to the greater surface area and the number of particles present at the same NP mass.[37]

Environmental Toxicology, Vol 35, No. 1 (January 2016): pg. 134-143. DOI.

The observed inhibition of cell metabolic activity rate but no impact on cell viability on exposure up to 480 mg/mL CuO NPs suggests that *S. cerevisiae* might use a mechanism such as cell cycle arrest, as found in human epithelial A549 cells,[40] to escape cell death. Copper is a redox active chemical involved in reactions leading to oxidative stress in cells. At the same time, Cu is eliciting antioxidant activity by acting as a redox site in superoxide dismutase (SOD1) for dismutating superoxide radicals. *Saccharomyces cerevisiae* is a great model to study how CuO NPs and the released Cu^{2+} influence these processes and further experimental work needs to be pursued. The specific pathways involved in *S. cerevisiae* response to sublethal concentrations of CuO NPs will be further studied by whole genome analyses.

Conclusion

The present study shows that under the tested conditions, CuO NPs had lesser effect on *S. cerevisiae* metabolic activity compared with Cu salts. However, the observed inhibition from the NPs was not fully explained by the released Cu ions from the dissolving NPs. The presence of a NP size effect may be related to the different physicochemical characteristics rather than only size. The present study also demonstrated a greater CuO NP effect on the metabolic activity of *S. cerevisiae* grown under respiring conditions. Future work in yeast should focus on the possible different impacts on metabolic pathways involved in respiring and fermenting cells and determine differences in cell response related to the nanostructure compared with dissolved soluble metals.

Acknowledgment

K.R. Hristova, A.D. Kappell, and M.J. Mashock conceived and designed the experiments. M.J. Mashock performed the experiments. N. Hallaj performed optimization of initial experiments. K.R. Hristova contributed materials, reagents, strains, and tools for analysis. The manuscript was prepared by M.J. Mashock, A.D. Kappell, and K.R. Hristova. Funding from Marquette University and the Children's Environmental Health Science Core Center, National Institute of Environmental Health Sciences grant number ES-04184 supported the present study. We thank D. Robertson and M. Gajdardziska-Josifovska,

University of Wisconsin at Milwaukee for the high-resolution transmission electron microscopy imaging and analysis.

Data availability

Data, associated metadata, and calculation tools are available from the author (krassimira.hristova@marquette.edu).

References

1 Rubilar O, Rai M, Tortella G, Diez MC, Seabra AB, Duran N. 2013. Biogenic nanoparticles: Copper, copper oxides, copper sulphides, complex copper nanostructures and their applications. *Biotechnol Lett* 35:1365–1375.

2 Miyazaki J, Kuriyama Y, Miyamoto A, Tokumoto H, Konishi Y, Nomura T. 2014. Adhesion and internalization of functionalized polystyrene latex nanoparticles toward the yeast *Saccharomyces cerevisiae. Adv Powder Technol* 25:1394–1397.

3 Aruoja V, Dubourguier HC, Kasemets K, Kahru A. 2009. Toxicity of nanoparticles of CuO, ZnO and TiO_2 to microalgae *Pseudokirchneriella subcapitata. Sci Total Environ* 407:1461–1468.

4 Ivask A, Bondarenko O, Jepihhina N, Kahru A. 2010. Profiling of the reactive oxygen species-related ecotoxicity of CuO, ZnO, TiO_2, silver and fullerene nanoparticles using a set of recombinant luminescent Escherichia coli strains: Differentiating the impact of particles and solubilized metals. *Anal Bioanal Chem* 398:701–716.

5 Kasemets K, Ivask A, Dubourguier HC, Kahru A. 2009. Toxicity of nanoparticles of ZnO, CuO and TiO_2 to yeast *Saccharomyces cerevisiae. Toxicol In Vitro* 23:1116–1122.

6 Kasemets K, Suppi S, Kunnis-Beres K, Kahru A. 2013. Toxicity of CuO nanoparticles to yeast Saccharomyces cerevisiae BY4741 wild-type and its nine isogenic single-gene deletion mutants. *Chem Res Toxicol* 26:356–367.

7 Mortimer M, Kasemets K, Kahru A. 2010. Toxicity of ZnO and CuO nanoparticles to ciliated protozoa *Tetrahymena thermophila. Toxicology* 269:182–189.

8 Heinlaan M, Kahru A, Kasemets K, Arbeille B, Prensier G, Dubourguier HC. 2011. Changes in the *Daphnia magna* midgut

upon ingestion of copper oxide nanoparticles: A transmission electron microscopy study. *Water Res* 45:179–190.

9 Zhao J, Wang ZY, Liu XY, Xie XY, Zhang K, Xing BS. 2011. Distribution of CuO nanoparticles in juvenile carp *(Cyprinus carpio)* and their potential toxicity. *J Hazard Mater* 197:304–310.

10 Suppi S, Kasemets K, Ivask A, Kunnis-Beres K, Sihtmae M, Kurvet I, Aruoja V, Kahru A. 2015. A novel method for comparison of biocidal properties of nanomaterials to bacteria, yeasts and algae. *J Hazard Mater* 286:75–84.

11 Gaggelli E, Kozlowski H, Valensin D, Valensin G. 2006. Copper homeostasis and neurodegenerative disorders (Alzheimer's, Prion, and Parkinson's diseases and Amyotrophic Lateral Sclerosis). *Chem Rev* 106:1995–2044.

12 Sumner ER, Avery AM, Houghton JE, Robins RA, Avery SV. 2003. Cell cycle- and age-dependent activation of Sod1p drives the formation of stress resistant cell subpopulations within clonal yeast cultures. *Mol Microbiol* 50:857–870.

13 Sousa VS, Teixeira MR. 2013. Aggregation kinetics and surface charge of CuO nanoparticles: The influence of pH, ionic strength and humic acids. *Environ Chem* 10:313–322.

14 Manusadzianas L, Caillet C, Fachetti L, Gylyte B, Grigutyte R, Jurkoniene S, Karitonas R, Sadauskas K, Thomas F, Vitkus R, Ferard JF. 2012. Toxicity of copper oxide nanoparticle suspensions to aquatic biota. *Environ Toxicol Chem* 31:108–114.

15 Sun M, Yu Q, Hu M, Hao Z, Zhang C, Li M. 2014. Lead sulfide nanoparticles increase cell wall chitin content and induce apoptosis in *Saccharomyces cerevisiae. J Hazard Mat* 273:7–16.

16 Gunawan C, Teoh WY, Marquis CP, Amal R. 2011. Cytotoxic origin of copper(II) oxide nanoparticles: Comparative studies with micron-sized particles, leachate, and metal salts. *ACS Nano* 5:7214–7225.

17 Sabel CE, Neureuther JM, Siemann S. 2010. A spectrophotometric method for the determination of zinc, copper, and cobalt ions in metalloproteins using Zincon. *Anal Biochem* 397:218–226.

18 Arzul G, Quiniou F, Carrie C. 2006. In vitro test-based comparison of pesticide-induced sensitivity in marine and freshwater phytoplankton. *Toxicol Mech Method* 16:431–437.

19 Conway JR, Adeleye AS, Gardea-Torresdey J, Keller AA. 2015. Aggregation, dissolution, and transformation of copper nanoparticles in natural waters. *Environ Sci Tech* 49:2749–2756.

20 Studer AM, Limbach LK, Van Duc L, Krumeich F, Athanassiou EK, Gerber LC, Moch H, Stark WJ. 2010. Nanoparticle cytotoxicity depends on intracellular solubility: Comparison of stabilized copper metal and degradable copper oxide nanoparticles. *Toxicol Lett* 197:169–174.

21 Karlsson HL, Cronholm P, Hedberg Y, Tornberg M, De Battice L, Svedhem S, Wallinder IO. 2013. Cell membrane damage and protein interaction induced by copper containing nanoparticles: Importance of the metal release process. *Toxicology* 313:59–69.

22 Karlsson HL, Gustafsson J, Cronholm P, Moller L. 2009. Size-dependent toxicity of metal oxide particles—a comparison between nano- and micrometer size. *Toxicol Lett* 188:112–118.

23 Shannahan JH, Lai X, Ke PC, Podila R, Brown JM, Witzmann FA. 2013. Silver nanoparticle protein corona composition in cell culture media. *PLoS One* 8:e74001.

24 Li M, Lin D, Zhu L. 2013. Effects of water chemistry on the dissolution of ZnO nanoparticles and their toxicity to *Escherichia coli. Environmental Pollution* 173:97–102.

25 Ansari AA, Naziruddin Khan M, Alhoshan M, Aldwayyan AS, Alsalhi MS. 2010. Nanostructured materials: Classification, properties, fabrication, characterization and their applications in biomedical sciences. In Kestell AE, DeLorey GT, eds, Nanoparticles: Properties, Classification, Characterization, and Fabrication. Nova Science Publishers, Hauppauge, NY, pp 1–78.

26 Adam N, Vakurov A, Knapen D, Blust R. 2015. The chronic toxicity of CuO nanoparticles and copper salt to *Daphnia magna. J Hazard Mat* 283:416–422.

27 Mahmoudi M, Serpooshan V. 2011. Large protein absorptions from small changes on the surface of nanoparticles. *J Phys Chem C* 115:18275–18283.

28 Ohno T, Sarukawa K, Matsumura M. 2002. Crystal faces of rutile and anatase TiO_2 particles and their roles in photocatalytic reactions. *New J Chem* 26:1167–1170.

29 Auffan M, Rose J, Wiesner MR, Bottero JY. 2009. Chemical stability of metallic nanoparticles: A parameter controlling their potential cellular toxicity in vitro. *Environ Poll* 157:1127–1133.

30 Oberdorster G, Kane AB, Klaper RD, Hurt RH. 2013. Nanotoxicity. In Klaassen CD, ed, Casarett and Doull's Toxicology: The Basic Science of Poisons. McGraw-Hill, New York, pp 1189–1229.

31 Wright M. 2012. Nanoparticle tracking analysis for the multiparameter characterization and counting of nanoparticle suspensions. In Soloviev M, ed, Nanoparticles in Biology and Medicine, Vol 906, Methods in Molecular Biology. Humana Press, New York, NY, USA, pp 511–524.

32 Franklin NM, Rogers NJ, Apte SC, Batley GE, Gadd GE, Casey PS. 2007. Comparative toxicity of nanoparticulate ZnO, bulk ZnO, and $ZnCl_2$ to a freshwater microalga *(Pseudokirchneriella subcapitata):* The importance of particle solubility. *Environ Sci Technol* 41:8484–8490.

33 Brunner TJ, Wick P, Manser P, Spohn P, Grass RN, Limbach LK, Bruinink A, Stark WJ. 2006. In vitro cytotoxicity of oxide nanoparticles: Comparison to asbestos, silica, and the effect of particle solubility. *Environ Sci Technol* 40:4374–4381.

34 Baek Y-W, An Y-J. 2011. Microbial toxicity of metal oxide nanoparticles (CuO, NiO, ZnO, and Sb_2O_3) to *Escherichia coli, Bacillus subtilis,* and *Streptococcus aureus. Sci Total Environ* 409:1603–1608.

35 Li L, Fernández-Cruz ML, Connolly M, Schuster M, Navas JM. 2015. Dissolution and aggregation of Cu nanoparticles in culture media: Effects of incubation temperature and particles size. *J Nano Res* 17:1–11.

36 Borm P, Klaessig FC, Landry TD, Moudgil B, Pauluhn J, Thomas K, Trottier R, Wood S. 2006. Research strategies for safety evaluation of nanomaterials, V: Role of dissolution in biological fate and effects of nanoscale particles. *Toxicol Sci* 90:23–32.

37 Oberdorster G, Oberdorster E, Oberdorster J. 2005. Nanotoxicology: An emerging discipline evolving from studies of ultrafine particles. *Environ Health Persp* 113:823–839.

38 Smith MR, Boenzli MG, Hindagolla V, Ding J, Miller JM, Hutchison JE, Greenwood JA, Abeliovich H, Bakalinsky AT. 2013. Identification of gold nanoparticle-resistant mutants of *Saccharomyces cerevisiae* suggests a role for respiratory

metabolism in mediating toxicity. *Applied Environ Micro* 79:728–733.

39 Heinlaan M, Ivask A, Blinova I, Dubourguier HC, Kahru A. 2008. Toxicity of nanosized and bulk ZnO, CuO and TiO_2 to bacteria *Vibrio fischeri* and crustaceans *Daphnia magna* and *Thamnocephalus platyurus. Chemosphere* 71:1308–1316.

40 Xu M, Fujita D, Sagisaka K, Watanabe E, Hanagata N. 2011. Production of extended single-layer graphene. *ACS Nano* 5:1522–1528.

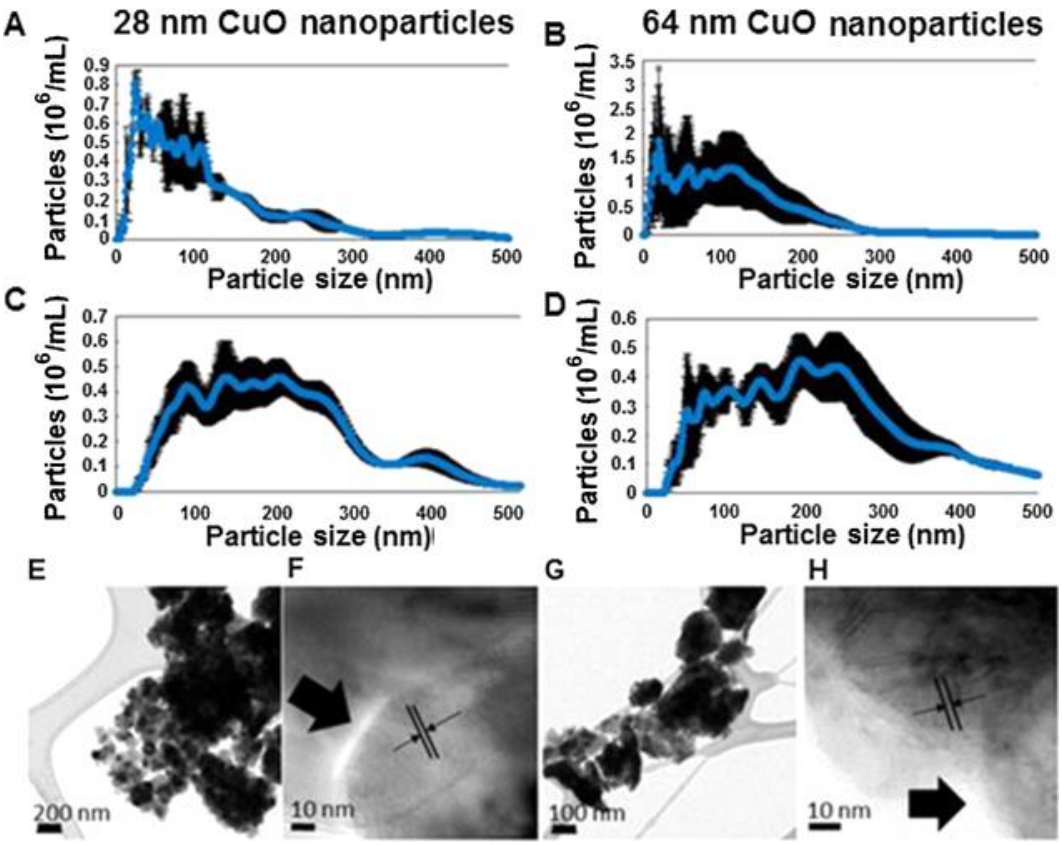

Figure 1. The 2 types of copper oxide nanoparticles (CuO NPs) have similar agglomeration in culture medium but different primary particle diameter and crystalline structures. The hydrodynamic size distribution was performed in ddH_2O (**A, B**) and YP-galactose (**C, D**) using nanoparticle tracking analysis (NTA). The 28 nm CuO NPs (**A, C**) tend to have smaller hydrodynamic diameters compared to 64 nm CuO NPs (**B, D**). All of the particles agglomerated in YP-galactose medium as seen by the size and position of the density distribution peaks in (**C**) and (**D**) compared to (**A**) and (**B**). Transmission electron microscopy (TEM) images of the CuO NPs indicate rough surfaces (indicated by large arrows) and show the primary diameter of the particles is different from that suggested by the manufacturers (**E–H**). High-resolution TEM images for 28 nm (**F**) and 64 nm (**H**) CuO NPs suggest different crystalline structures

for the 2 NPs. The different lattice fringe width is highlighted for easier observation by parallel lines with small arrows.

Table 1. Cu^{2+} released from copper oxide nanoparticles in growth media

	Conc. (mg/L)	1.5 h[a]	5.5 h	25.5 h
28 nm copper oxide nanoparticles				
YP-galactose	40	0.95 ± 0.11	2.54 ± 0.15	8.67 ± 1.40
	80	0.93 ± 0.51	5.35 ± 0.53	22.35 ± 1.7
	240	6.98 ± 1.0	10.62 ± 0.22	101.1 ± 15.0
ddH_2O	40	BDL	BDL	BDL
	80	BDL	BDL	BDL
	240	BDL	BDL	BDL
64 nm copper oxide nanoparticles				
YP-galactose	40	0.34 ± 0.08	0.59 ± 0.07	0.79 ± 0.07
	80	0.71 ± 0.08	0.83 ± 0.02	1.36 ± 0.03
	240	1.96 ± 0.06	2.56 ± 0.13	3.66 ± 0.4
ddH_2O	40	BDL	BDL	BDL
	80	BDL	BDL	0.17 ± 0.02
	240	BDL	BDL	0.32 ± 0.04

Data are mean of 3 replicates of 2 independent experiments ± range of values.
BDL = Below detection limit of Zincon assay (0.24 mg/L).
a Period of time nanoparticles were incubated in media or water.

Table 2. *Saccharomyces cerevisiae* cell metabolic rate IC50 values of 1.5 h copper exposure in YP media with selected carbon sources

	28 nm copper oxide nanoparticles	64 nm copper oxide nanoparticles	$CuSO_4$
YP-Dextrose	305 ± 67.2	468 ± 27.2	10.3 ± 2.0
YP-Glycerol	224 ± 30.4	304 ± 38.4	5.3 ± 2.3
YP-EtOH	96 ± 23.0	224 ± 52.0	2.7 ± 0.1
YP-Galactose	88 ± 15.2	216 ± 17.6	2.4 ± 0.5

1. IC50 = The concentration of the copper compound that reduced cell metabolic activity by 50%.

Environmental Toxicology, Vol 35, No. 1 (January 2016): pg. 134-143. DOI.

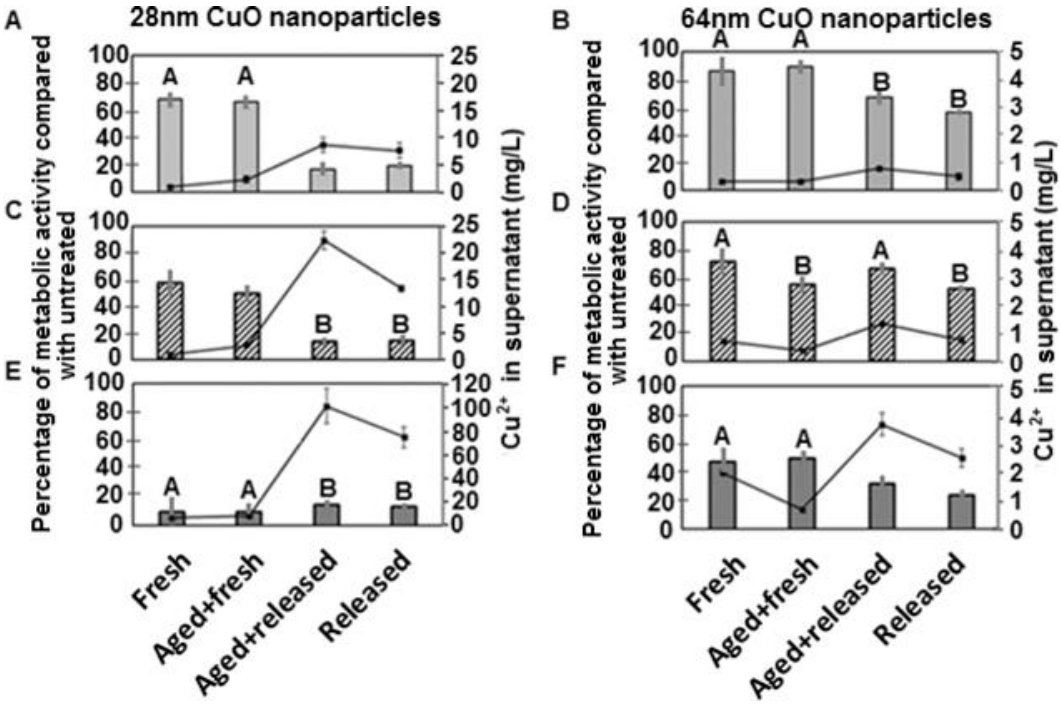

Figure 2. Nanoparticle (NP) exposure scenarios with high concentrations of released Cu^{2+} inhibit *Saccharomyces cerevisiae* W303-1A metabolism to a greater extent compared to fresh NP suspensions. Inhibition of cellular metabolic activity rate after 1.5 h exposure to 28 nm (**A, C, E**) or 64 nm copper oxide (CuO) NPs (**B, D, F**). Copper oxide NPs effect was assessed using aB assay at 40 mg/L (**A, B**), 80 mg/L (**C, D**) and 240 mg/L (**E, F**). The bar graph represents results expressed as percentage of metabolic activity compared to untreated cells. The line graph represents Cu^{2+} ions released into YP-galactose medium from each respective treatment. Results are presented as mean ± standard deviation of 3 independent experiments. Significant results as compared to the other treatments (bar graph, $p < 0.05$) are marked with letters, values with the same letter indicate they are not significantly different from one another. Error bars represent standard deviation.

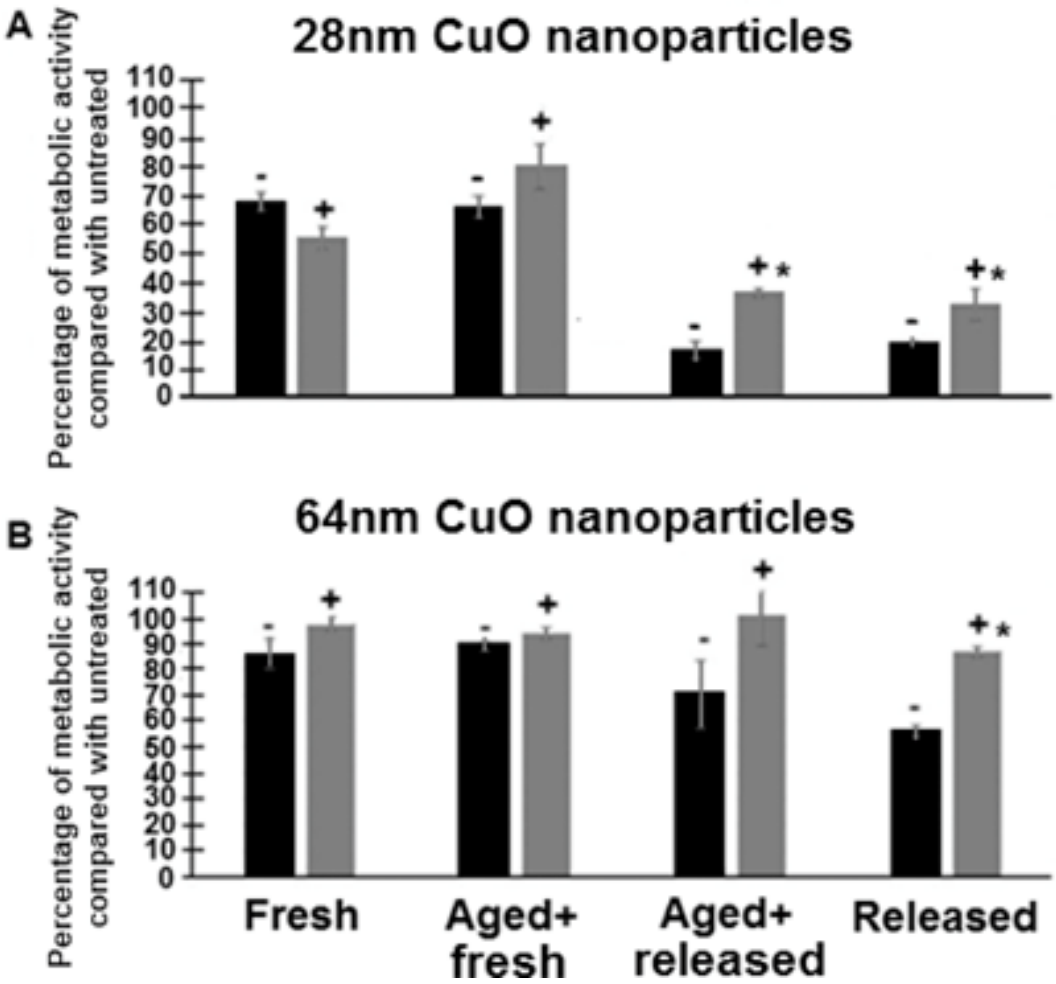

Figure 3. Copper ion chelation impacts copper oxide nanoparticle (CuO NP) inhibition on *Saccharomyces cerevisiae* W303-1A metabolic activity rate. Nanoparticles effect on *S. cerevisiae* metabolism after 1.5 h exposure at 40 mg/L of 28 nm (**A**) or 64 nm (**B**) CuO NPs was assessed using aB assay. Black bars represent treatment without chelation (−) and grey bars represent treatment with the addition of ethylenediaminetetraacetic acid (EDTA) at 0.5 mM (+). Data are expressed as percentage of metabolic activity compared to untreated cells. Error bars represent standard deviation of 3 independent experiments. Significant differences between treatments without chelation (−) compared to treatment with EDTA (+) are indicated with an asterisk ($p < 0.05$).

Supplemental Data

The Supplemental Data are available on the Wiley Online Library at DOI: 10.1002/etc.3159.

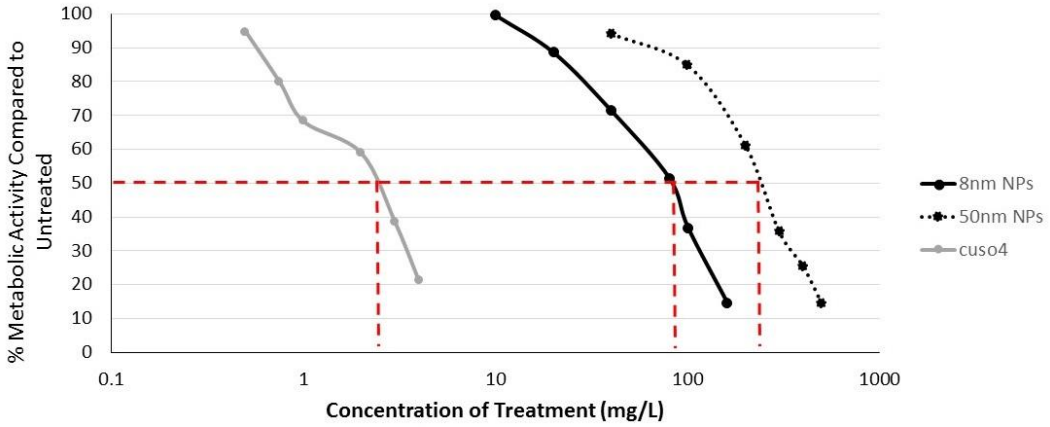

Figure S1. Comparison of IC_{50} values of metabolic activity rate for tested 28 nm and 64 nm copper oxide nanoparticles. Red lines indicate IC_{50} value for respective copper exposure scenarios.

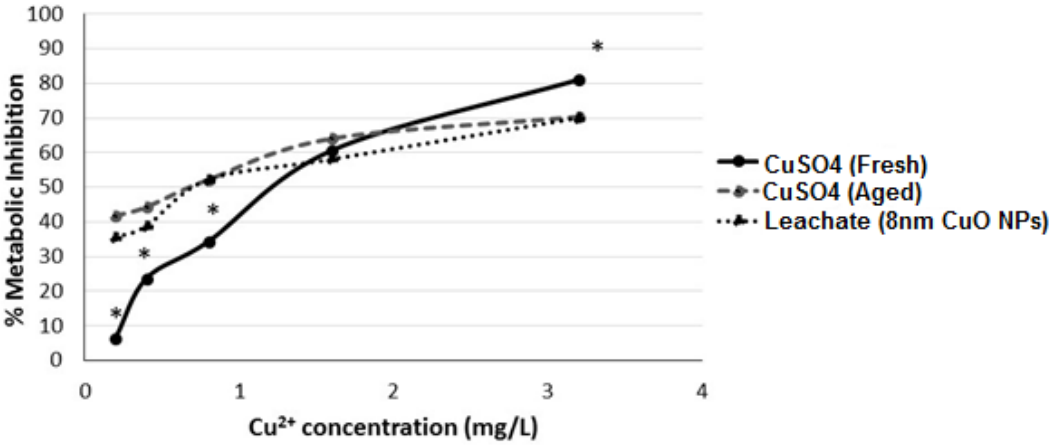

Figure S2. Copper sulfate more closely mimics the inhibitory effect of nanoparticle released fraction when allowed to interact with the yeast growth media. 8 nm CuO NPs and CuSO4 were added to sterile YP-Gal media for 24h and then diluted to 0.2-3.2 mg/L Cu^{2+} and inhibition of metabolic activity was assayed after 1.5h exposure. Significant difference ($p<0.05$) is indicated by asterisks.

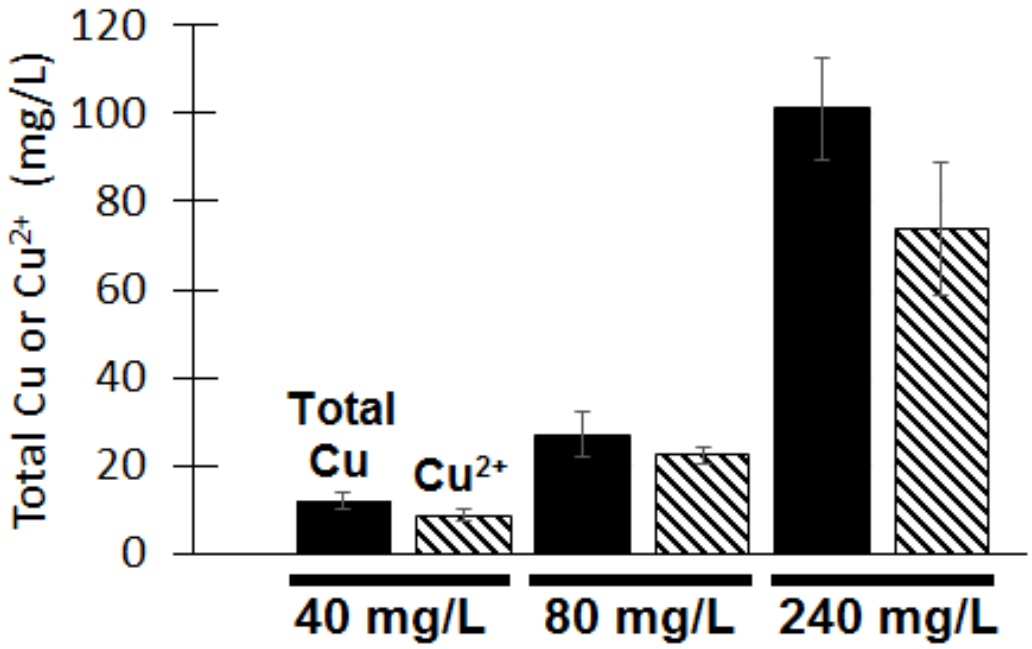

Figure S3. Characterization of the released fraction from CuO nanoparticle incubation in growth media. CuO nanoparticle released fraction contains predominantly a population of Cu^{2+} ions. 8nm CuO nanoparticles were aged for 24h in sterile YP growth media, nanoparticles were removed from solution by ultracentrifugation, and supernatant was then assayed for total copper (solid bars) or Cu^{2+} ions (stripped bars). There was no statistically significant difference between the total Cu and Cu^{2+} concentrations for 40, 80, and 240 mg/L treatments (p-value 0.053, 0.061, and 0.098, respectively).

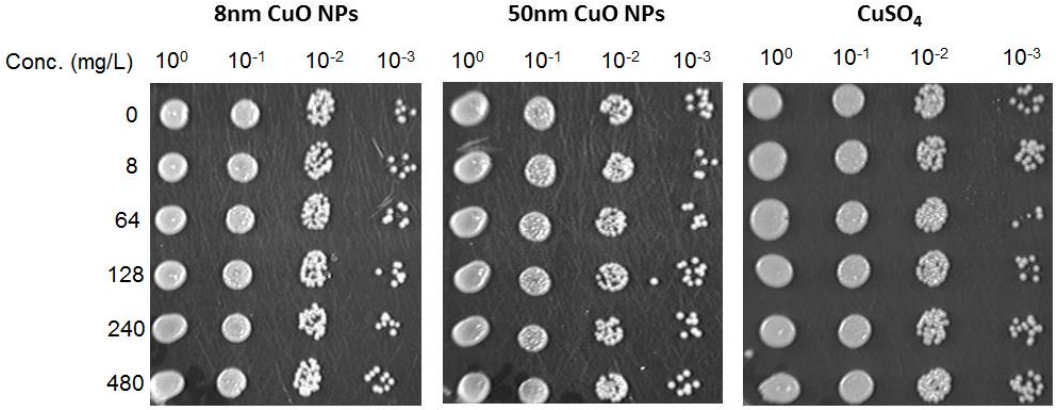

Figure S4. Neither copper oxide nanoparticles nor copper sulfate have an effect on *S. cerevisiae* cell viability at the selected doses of exposure. Images are representative of spot assays performed on agar plates with all carbon sources (dextrose, glycerol, and galactose) and at different time of exposure (1.5h, 24h, and 48h). Cell suspensions were serially diluted and incubated on agar plates for 72h at 30°C.

Table S1. Characterization of copper oxide nanoparticles and their properties when suspended in media or water

Average hydrodynamic diameter (nm)			
8nm copper oxide nanoparticles			
Experimental media	**1.5h[a]**	**5.5h**	**25.5h**
YP-Galactose	214 ± 112	184 ± 116	222 ± 141
YP-EtOH	200 ± 162	225 ± 117	236 ± 129
ddH_2O	87 ± 7	191 ± 175	113 ± 82
50nm copper oxide nanoparticles			
YP-Galactose	240 ± 172	124 ± 48	211 ± 155
YP-EtOH	346 ± 177	232 ± 182	175 ± 104
ddH_2O	144 ± 149	140 ± 90	160 ± 94
Zeta-potential (mV)			
8nm copper oxide nanoparticles			
Experimental media	**1.5h**	**5.5h**	**25.5h**
YP-Galactose	-14.5 ± 0.5	-10.5 ± 0.2	-7.8 ± 0.3
YP-EtOH	-14.5 ± 0.5	-10.4 ± 0.6	-9.2 ± 0.1
ddH_2O	-13.9 ± 0.7	-15.2 ± 7.2	-21.2 ± 5.9
50nm copper oxide nanoparticles			
YP-Galactose	-12.8 ± 0.3	-5.6 ± 0.7	-8.6 ± 0.4
YP-EtOH	-12.8 ± 0.3	-9.7 ± 0.3	-8.9 ± 0.8
ddH2O	-12.7 ± 0.4	-16.6 ± 6.4	-11 ± 11.1

Data are mean of 3 replicates of 2 independent experiments ± range of values.
[a] Period of time nanoparticles were incubated in media or water.

Table S2. Percent metabolic rate of *S. cerevisiae* cells after copper exposure

8nm copper oxide nanoparticle exposure scenarios					
	Concn. (mg/L)	**Fresh NPs in Fresh Media**	**Aged NPs in Fresh Media**	**Aged NPs in Released Fraction**	**Released Fraction**
Without EDTA	40	68.1+/-9.2	66.0+/-3.8	16.7+/-2.9	19.2+/-0.5
	80	57.6+/-3.2	49.5+/-5.2	13.2+/-2.1	13.8+/-2.6
	240	9.9+/-5.1	9.3+/-0.6	14.3+/-0.5	13.2+/-1.2
With EDTA[a]	40	55.2+/-3.5	79.7+/-7.7	36.4+/-1.5	32.4+/-5.4
	80	36.0+/-1.1	66.2+/-6.6	13.1+/-1.2	13.9+/-1.3
	240	5.8+/-0.3	20.3+/-9.3	10.2+/-4.9	14.8+/-3.4
50nm copper oxide nanoparticle exposure scenarios					

Environmental Toxicology, Vol 35, No. 1 (January 2016): pg. 134-143. DOI.

	Concn. (mg/L)	Fresh NPs Fresh Media	Aged NPs Fresh Media	Aged NPs in Released Fraction	Released Fraction
Without EDTA	40	85.8+/-5.6	89.2+/-2.0	70.0+/-13.0	56.3+/-2.1
	80	71.7+/-6.3	54.9+/-4.1	66.5+/-0.6	52.1+/-6.8
	240	46.8+/-1.8	49.3+/-6.9	31.7+/-7.8	23.5+/-0.4
With EDTA	40	97.2+/-2.6	93.7+/-2.2	101.1+/-12	86.5+/-2.1
	80	82.3+/-2.9	80.3+/-2.6	79.6+/-2.5	84.9+/-2.5
	240	60.7+/-5.7	60.8+/-0.3	57.9+/-3.6	61.3+/-2.3

Results are expressed as percent metabolic activity of *S. cerevisiae* compared to untreated cells. Data are mean of 3 replicates of 2 independent experiments ± range of values.

[a] 0.5 mM EDTA added 1h prior to addition of cells

NPs = nanoparticles